



TITLE:

MYC Releases Early Reprogrammed Human Cells from Proliferation Pause via Retinoblastoma Protein Inhibition

AUTHOR(S):

Rand, Tim A.; Sutou, Kenta; Tanabe, Koji; Jeong, Daeun; Nomura, Masaki; Kitaoka, Fumiyo; Tomoda, Emi; ... Rulifson, Eric; Yamanaka, Shinya; Takahashi, Kazutoshi

CITATION:

Rand, Tim A. ...[et al]. MYC Releases Early Reprogrammed Human Cells from Proliferation Pause via Retinoblastoma Protein Inhibition. Cell Reports 2018, 23(2): 361-375

ISSUE DATE:

2018-04-10

URL:

<http://hdl.handle.net/2433/230952>

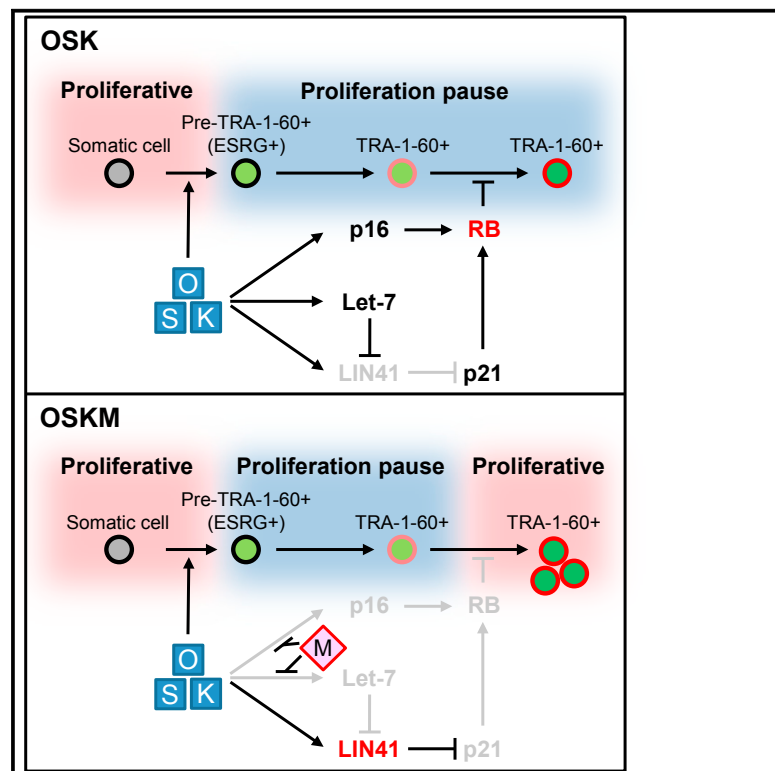
RIGHT:

© 2018 The Authors. This is an open access article under the CC BY-NC-ND license (<http://creativecommons.org/licenses/by-nc-nd/4.0/>).

Cell Reports

MYC Releases Early Reprogrammed Human Cells from Proliferation Pause via Retinoblastoma Protein Inhibition

Graphical Abstract



Authors

Tim A. Rand, Kenta Sutou, Koji Tanabe, ..., Eric Rulifson, Shinya Yamanaka, Kazutoshi Takahashi

Correspondence

syamanaka@gladstone.ucsf.edu (S.Y.), kazutoshi.takahashi@gladstone.ucsf.edu (K.T.)

In Brief

Rand et al. find that MYC promotes proliferation of human intermediate reprogrammed cells rather than initiation of reprogramming. MYC post-transcriptionally activates LIN41, resulting in post-transcriptional suppression of p21. Suppression of p21 results in reduction of RB activity, which is a negative regulator of reprogramming progression.

Highlights

- ESRG (+) early reprogramming cells do not proliferate due to RB activation
- MYC does not facilitate appearance of ESRG (+) cells but induces their proliferation
- MYC inactivates RB by suppressing p16 and p21, with the latter mediated through LIN41
- Immortalized cells show efficient reprogramming without exogenous MYC

Data and Software Availability

GSE89455
GSE90015



MYC Releases Early Reprogrammed Human Cells from Proliferation Pause via Retinoblastoma Protein Inhibition

Tim A. Rand,^{1,6} Kenta Sutou,^{2,6} Koji Tanabe,³ Daeun Jeong,¹ Masaki Nomura,² Fumiyo Kitaoka,² Emi Tomoda,¹ Megumi Narita,² Michiko Nakamura,² Masahiro Nakamura,² Akira Watanabe,² Eric Rulifson,⁴ Shinya Yamanaka,^{1,2,5,*} and Kazutoshi Takahashi^{1,2,7,*}

¹Gladstone Institute of Cardiovascular Disease, San Francisco, CA 94158, USA

²Department of Life Science Frontiers, Center for iPS Cell Research and Application, Kyoto University, Kyoto 606-8507, Japan

³Institute for Stem Cell Biology and Regenerative Medicine and Department of Pathology, Stanford University School of Medicine, Stanford, CA 94305, USA

⁴Department of Developmental Biology, Stanford University School of Medicine, Stanford, CA 94305, USA

⁵Department of Anatomy, University of California, San Francisco, San Francisco, CA 94143, USA

⁶These authors contributed equally

⁷Lead Contact

*Correspondence: syamanaka@gladstone.ucsf.edu (S.Y.), kazutoshi.takahashi@gladstone.ucsf.edu (K.T.)

<https://doi.org/10.1016/j.celrep.2018.03.057>

SUMMARY

Here, we report that MYC rescues early human cells undergoing reprogramming from a proliferation pause induced by OCT3/4, SOX2, and KLF4 (OSK). We identified ESRG as a marker of early reprogramming cells that is expressed as early as day 3 after OSK induction. On day 4, ESRG positive (+) cells converted to a TRA-1-60 (+) intermediate state. These early ESRG (+) or TRA-1-60 (+) cells showed a proliferation pause due to increased p16INK4A and p21 and decreased endogenous MYC caused by OSK. Exogenous MYC did not enhance the appearance of initial reprogramming cells but instead reactivated their proliferation and improved reprogramming efficiency. MYC increased expression of LIN41, which potently suppressed p21 post-transcriptionally. MYC suppressed p16 INK4A. These changes inactivated retinoblastoma protein (RB) and reactivated proliferation. The RB-regulated proliferation pause does not occur in immortalized fibroblasts, leading to high reprogramming efficiency even without exogenous MYC.

INTRODUCTION

Enforced expression of specific transcription factors (OCT3/4, SOX2, KLF4, and MYC, abbreviated as OSKM) reprograms somatic cells toward pluripotency (Takahashi et al., 2007; Takahashi and Yamanaka, 2006). These factors induce dynamic changes in gene expression, such as the suppression of somatic cell genes and activation of pluripotency-associated genes (Buganim et al., 2013). Initially, all four factors were thought to be essential for reprogramming. However, exogenous MYC is dispensable, even though it greatly enhances the efficiency of re-

programming by OCT3/4, SOX2, and KLF4 (OSK) (Nakagawa et al., 2008; Wernig et al., 2008). Many factors promote OSK-mediated reprogramming, but MYC remains one of the strongest activators of induced pluripotent stem cell (iPSC) generation.

MYC was one of the first proto-oncogenes identified in humans more than 30 years ago (Hayward et al., 1981; Vennstrom et al., 1982). Overexpression of MYC is a hallmark associated with up to 70% of all human cancers (Ciriello et al., 2013; Dang, 2012; Gabay et al., 2014). It belongs to a basic helix-loop-helix-leucine-zipper (bHLH-Zip) family of transcription factors and requires the partner protein MAX to bind canonical E-box elements (CACGTG) or other non-canonical variants (CANNTG) (Blackwell et al., 1990; Blackwood and Eisenman, 1991; Lin et al., 2012). MYC primarily functions as a transcription activator through interaction with other activators, such as histone acetyltransferases and Mediator (Vervoorts et al., 2003). However, MYC can also function as a transcriptional suppressor by interacting with other partners, such as MIZ1 and polycomb repressive complex (PRC) 2 (Haupt et al., 1991; Peukert et al., 1997; van Lohuizen et al., 1991). In addition, MYC may function as a universal amplifier of expressed genes (Lin et al., 2012; Wolf et al., 2015).

MYC is involved in various biological processes. It stimulates the cell cycle by promoting DNA synthesis (Dominguez-Sola and Gautier, 2014). It alters metabolism from oxidative phosphorylation to glycolysis, the latter of which is active in pluripotent stem cells and cancer cells (Cliff et al., 2017; Dang, 2013, 2015; Folmes et al., 2013). MYC also activates non-coding RNAs, including microRNAs (miRNAs), such as miR17-miR92 expression in mouse embryonic stem cells (ESCs) (Lin et al., 2009; Smith et al., 2010). MYC regulates, and in many cases suppresses, developmental genes such as GATA6 and HOX genes (Chappell and Dalton, 2013). In addition, MYC affects signaling pathways. For example, MYC suppresses the ERK/mitogen-activated protein kinase (MAPK) pathway through DUSP2/7, whereas it activates the Wnt pathway through PRC2 (Chappell et al., 2013; Fagnocchi et al., 2016). Moreover, MYC can induce



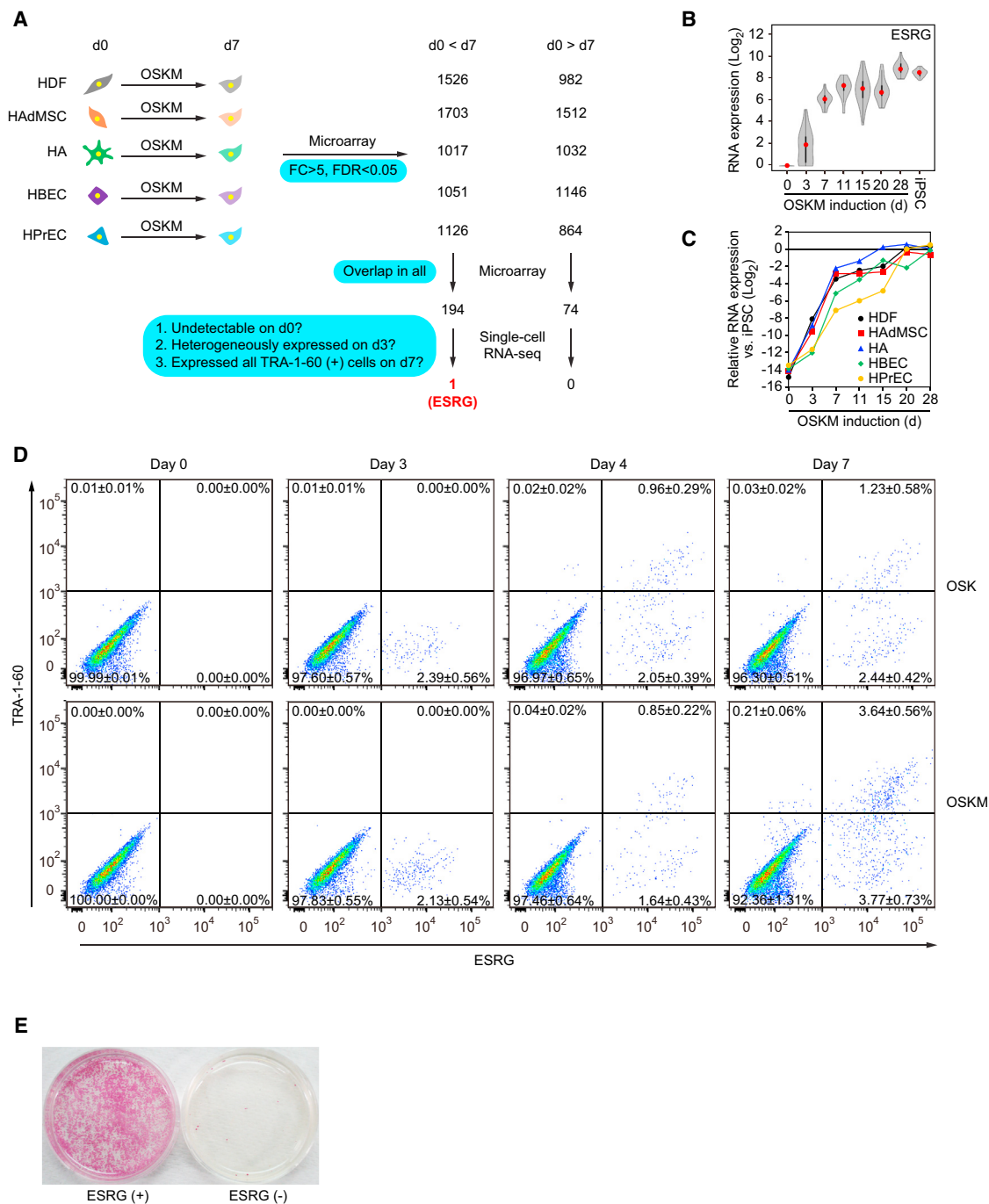


Figure 1. Identifying the Early Marker of Reprogramming

(A) Extraction of commonly changed genes and narrowing of the candidates for reprogramming marker. We used microarrays to compare global gene expression of somatic cells (HDFs, HAdMSCs, HAs, HBECs, and HPrECs) on day 0 (d0) and their TRA-1-60 (+) progenies on day 7 (d7) post-transduction of OSKM. $n = 3$. By comparing differentially expressed genes between parental cells and TRA-1-60 (+) cells among five cell types, we obtained the indicated common genes. These commonly changed genes were evaluated by single-cell RNA-seq to narrow down the candidates. Blue boxes show the criteria of analyses. See also [Tables S1](#) and [S2](#).

(B) Expression of ESRG during reprogramming. Shown are the results of expressing ESRG in parental HDFs (d0), OSKM-expressing cells on day 3 (d3), TRA-1-60 (+) cells at the indicated time points (days 7–28), and iPSCs analyzed by single-cell RNA-seq. Twenty-four single cells were analyzed for each time point. Red dots indicate median values. Gray hourglass shapes represent the distribution of the reads per kilobase of transcript, per million mapped reads (RPKM) + 1 value. See also [Figure S1](#).

(legend continued on next page)

global epigenomic changes that affect binding of other transcription factors and nuclear architecture (Kieffer-Kwon et al., 2017; Kress et al., 2015).

MYC facilitates early stages of reprogramming, but the molecular mechanism remains controversial (Polo et al., 2012; Soufi et al., 2012; Sridharan et al., 2009). It may enhance early steps of reprogramming by repressing fibroblast-specific gene expression and upregulating the metabolic program of the embryonic state (Sridharan et al., 2009). This paper also showed that exogenous MYC is required during the initial 5 days after OSK induction to promote iPSC generation. Alternatively, MYC may facilitate binding of OSK factors to their target genes in the first 48 hr of reprogramming (Soufi et al., 2012). Another study showed that MYC, together with KLF4, elicits the first wave of changes during reprogramming, including induction of proliferation, metabolic changes, and loss of genetic program of fibroblasts (Polo et al., 2012). Thus, how MYC promotes early stages of reprogramming remains unclear (Knoepfler, 2008).

In the current study, we used three unprecedented opportunities to clarify the role of MYC during reprogramming. First, we identified a specific marker of reprogramming that is activated as early as 3 days after OSKM introduction. This allowed us to examine the role of MYC in the early stages during human iPSC generation. Because only a small fraction of cells that receive OSK or OSKM can start reprogramming, data would be misleading without purification using a specific marker. Second, we generated teratoma-derived fibroblasts (TdFs) that reprogram as efficiently using OSK alone as with OSKM. Exogenous MYC did not enhance iPSC generation in this line. To our knowledge, this is the only identified cell line for which reprogramming is not enhanced by exogenous MYC. Therefore, TdFs provide a unique tool to help determine the role of MYC. Third, as we previously described, the heterochronic developmental factor LIN41/TRIM71, like MYC, enhances reprogramming when added to OSK (Worringer et al., 2014). Here, we provide a clear molecular mechanism by which LIN41 enhances reprogramming and demonstrate that this function is closely related to MYC; it is a critical downstream effector for MYC-enhancement of reprogramming. Collectively, our data show that MYC promotes human iPSC generation primarily by facilitating the escape of an OSK-induced proliferation blockade in early reprogramming cells. It does this by repressing retinoblastoma protein (RB) rather than enhancing OSK binding, suppressing fibroblast-specific genes, or inducing metabolic changes.

RESULTS

ESRG Is an Early Marker of Human Cellular Reprogramming

To understand what happens in the initial phase of reprogramming, we tried to identify markers that detect reprogramming

cells before TRA-1-60. We analyzed the global gene expression of five human somatic cell types—i.e., human dermal fibroblasts (HDFs, mesoderm), human adipose-derived mesenchymal stem cells (HADMSCs, mesoderm), human astrocytes (HAs, ectoderm), human bronchial epithelial cells (HBECs, endoderm), and human prostate epithelial cells (HPrECs, endoderm)—and their TRA-1-60 (+) reprogramming progenies on day 7 after introduction of OSKM (fold change [FC] > 5.0, false discovery rate [FDR] < 0.05) using gene expression arrays (Figure 1A). We identified 194 upregulated genes (Table S1) and 74 downregulated genes (Table S2) that were common in all five somatic cells. Known early reprogramming markers (e.g., L1TD1, SALL4, and NANOG) and other pluripotency-associated genes (e.g., TGDF1, DNMT3L, and ESRG) were among the upregulated genes (Buganim et al., 2012; O'Malley et al., 2013; Takahashi et al., 2014).

We expected some of the 194 commonly upregulated genes to function as early markers of reprogramming. We rationalized that good markers should fulfill the following criteria: (1) undetectable expression in somatic cells, (2) heterogeneous expression in cells on day 3, and (3) expression in all TRA-1-60 (+) cells on day 7 (Figure 1A). We used single-cell RNA sequencing (RNA-seq) to examine parental HDFs, OSKM-expressing cells on day 3, TRA-1-60 (+) cells on days 7–28, and iPSCs. This analysis revealed that only one gene, ESRG encoding a human endogenous retrovirus type H (HERV-H)-driven long non-coding RNA (lncRNA), fulfilled all three criteria (Figures 1A and 1B) (Li et al., 2013). We then examined the expression of ESRG during iPSC generation from the five types of somatic cells and confirmed similar expression patterns (Figure 1C). These data show that ESRG functions as an early marker of reprogramming toward human iPSCs regardless of starting somatic cell types.

To better monitor ESRG (+) cells, we generated an iPSC line carrying an ESRG-Clover allele by CRISPR/Cas9-mediated homologous recombination (Figures S1A–S1E). The resulting reporter clone revealed that undifferentiated iPSCs specifically and uniformly expressed Clover fluorescent proteins driven by the endogenous ESRG promoter (Figures S1F–S1H). We transduced OSK or OSKM into fibroblasts derived from ESRG-Clover iPSCs. Before transduction, fibroblasts expressed neither ESRG nor TRA-1-60 (Figures 1D and S1F–S1H). On day 3, we detected $2.39\% \pm 0.56\%$ and $2.13\% \pm 0.54\%$ of ESRG-Clover (+) cells after transduction of OSK and OSKM, respectively (Figure 1D). On day 3, we did not detect TRA-1-60 (+) cells, suggesting that ESRG is activated earlier than TRA-1-60 during reprogramming. On day 4, a small number ($0.96\% \pm 0.29\%$ by OSK and $0.85\% \pm 0.22\%$ by OSKM) of ESRG (+)/TRA-1-60 (+) cells emerged (Figure 1D). The proportion of ESRG (+) cells on day 4 did not significantly increase from that on day 3 (2.39% versus 3.01% by OSK and 2.49% versus 2.13% by OSKM) (Figure 1D). In addition, we used cell sorting to purify ESRG (+) cells on day 3. After

(C) Expression of ESRG during reprogramming. Shown is the expression of ESRG in parental cells (d0), OSKM-expressing cells on day 3 (d3), TRA-1-60 (+) cells at the indicated time points (days 7–28) derived from HDFs, and HADMSCs, HAs, HBECs, and HPrECs analyzed by microarray. $n = 3$.

(D) TRA-1-60 (+) cells emerged only from ESRG (+) cells. Shown are representative histograms of ESRG-Clover (x axis) and TRA-1-60 (y axis) expression in ESRG-Clover fibroblasts (day 0) and those on days 3, 5, and 7 post-transduction by OSK or OSKM. $n = 3$. See also Figure S1.

(E) ESRG (+) cells are origins of iPSCs. We introduced OSKM into ESRG-Clover fibroblasts by retroviral transduction and purified ESRG (+) and ESRG (–) cells by cell sorting. Sorted cells (100,000) were plated onto MMC-treated SNL feeder layers. A terminal stain was performed with red alkaline phosphatase on day 24. $n = 3$.

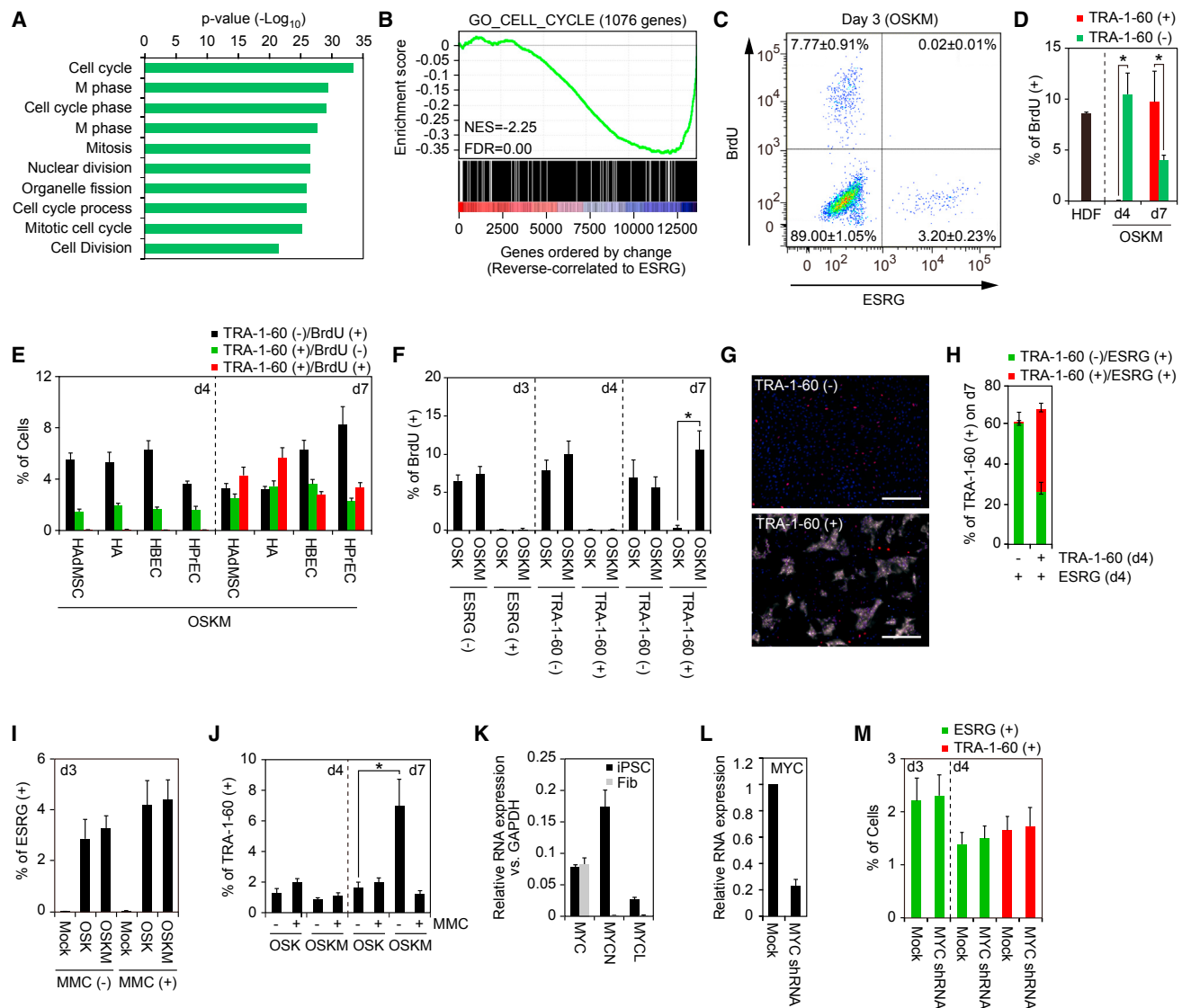


Figure 2. Cell-Cycle Progression Is Dispensable for Initiating Reprogramming

(A) Gene ontology analyses of genes varied according to ESRG. Top 200 genes reverse correlated to ESRG were classified by the gene ontology analysis. The p values of the top 10 enriched terms are shown. See also Table S3.

(B) Gene set enrichment analysis showing enrichment of cell-cycle-related genes in the set of genes that show reverse correlation with ESRG expression. x axis shows genes ranked by the Pearson correlation coefficient for ESRG expression. Left, positively correlated genes; right, negatively correlated genes. See also Table S3.

(C) Proliferation of ESRG (+) cells. Shown is a representative histogram of the BrdU incorporation of OSKM-transduced ESRG-Clover fibroblasts on day 3. n = 3.

(D) Proliferation of newly converted TRA-1-60 (+) cells from HDFs. Shown are the percentages of the BrdU incorporation of parental HDFs on day 0 (d0), TRA-1-60 (+) or TRA-1-60 (-) cells on day 4 (d4) or day 7 (d7). *p < 0.05 by unpaired t test (n = 3).

(E) Proliferation of newly converted TRA-1-60 (+) cells from other cell types. Shown are the percentages of TRA-1-60 (+)/BrdU (-) (black), TRA-1-60 (+)/BrdU (+) (red), or TRA-1-60 (-)/BrdU (+) cells on day 4 (d4) or day 7 (d7). n = 3.

(F) MYC enhances the proliferation of TRA-1-60 (+) cells. Shown are the percentages of BrdU (+) incorporation in ESRG (+) cells on day 3 (d3) and TRA-1-60 (+) cells on day 4 (d4) or day 7 (d7) induced by OSK or OSKM. *p < 0.05 by unpaired t test (n = 3).

(G) MYC does not enhance the continuity of TRA-1-60 conversion. Shown are representative immunocytochemistry images of the cells on day 7 derived from sorted TRA-1-60 (+) or TRA-1-60 (-) cells in the ESRG (+) population on day 4 post-transduction of OSKM stained with TRA-1-60 (white) and OCT3/4 (red) antibodies. Nuclei were visualized by Hoechst 33342 staining. Bars indicate 100 μ m.

(H) TRA-1-60 (-) cells on day 4 did not convert to a TRA-1-60 (+) fate. Shown are quantitative results of ESRG (+)/TRA-1-60 (+) cells (red) and ESRG (+)/TRA-1-60 (-) cells (green) in the cells shown in (G).

(I) Percentages of ESRG (+) cells from MMC-treated (+) or non-treated (-) ESRG-Clover fibroblasts on day 3 post-transduction of OSKM. n = 3. See also Figure S2.

(legend continued on next page)

re-plating, ESRG (+) cells produced many iPSC colonies, whereas ESRG (–) cells resulted in few (Figure 1E). These data demonstrate that TRA-1-60 (+) intermediate reprogramming cells and iPSCs emerged only from ESRG (+) cells.

Seven days after OSKM induction, the proportion of ESRG (+)/TRA-1-60 (+) cells and ESRG (+)/TRA-1-60 (–) cells rose to $3.64\% \pm 0.56\%$ and $3.77\% \pm 0.73\%$, respectively (Figure 1D). Thus, the ESRG population on day 7 increased 3-fold from that of day 4. ESRG (–)/TRA-1-60 (+) cells were practically zero by day 7 (Figure 1D), and OSK induced ESRG (+) cells on day 3 and TRA-1-60 (+) cells on day 4 comparable to OSKM (Figure 1D). However, without exogenous MYC, the proportion of ESRG (+)/TRA-1-60 (+) cells and ESRG (+)/TRA-1-60 (–) cells remained low on day 7 ($1.23\% \pm 0.58\%$ and $2.44\% \pm 0.52\%$, respectively). These data suggest that MYC does not facilitate initial emergence of ESRG and TRA-1-60 (+) cells but rather promotes expansion of early reprogramming cells between day 4 and day 7.

Early Reprogramming Cells Do Not Proliferate

To understand how MYC promotes expansion of early reprogramming cells, we examined gene expression at a single-cell level 3 days after transduction of OSKM into HDFs. By gene ontology (GO) analysis, genes with expression levels that showed reverse correlation with ESRG expression were significantly enriched with cell-cycle-related terms (Figure 2A; Table S3). Gene set enrichment analysis (GSEA) indicated that the expression levels of 612 of 1,076 cell-cycle-related genes showed reverse correlation to ESRG expression ($p = 1.95e-10$ by Fisher's exact test) (Figure 2B; Table S3). Based on these results, we next examined the proliferation profile of early reprogramming cells using bromodeoxyuridine (BrdU) incorporation. Three days after OSKM induction, BrdU (+) cells were readily detected in ESRG (–) cells, but not in ESRG (+) cells (Figure 2C). This was also the case with TRA-1-60 (+) cells and TRA-1-60 (–) cells on day 4 (Figure 2D). On day 7, BrdU (+) cells significantly increased in TRA-1-60 (+) cells and decreased in TRA-1-60 (–) cells (Figure 2D). Comparable results were observed in TRA-1-60 (+) cells on days 4 and 7 after OSKM induction into other types of somatic cells, including hAdMSCs, HAs, HBECs, and hPReCs (Figure 2E). These data demonstrated that ESRG (+) cells do not proliferate when they emerge at day 3 and convert to TRA-1-60 (+) cells at day 4 after OSKM induction, regardless of the origin of the somatic cells. By day 7 after OSKM transduction, however, early reprogramming cells initiate proliferation.

MYC Promotes Proliferation in Reprogramming Cells

We then determined whether proliferation in early reprogramming cells depends on exogenous MYC. We induced OSK or

OSKM and examined the proportion of TRA-1-60 (+) cells on days 4 and 7. The proportions of new TRA-1-60 (+) cells induced by OSK or OSKM on day 4 were comparable (Figure 1D). In contrast, on day 7, we observed increases in the proportion of TRA-1-60 (+) cells with OSKM, but not with OSK (Figure 1D). This tendency correlated well with BrdU incorporation into TRA-1-60 (+) cells (Figure 2F). ESRG (+) cells and TRA-1-60 (+) cells did not incorporate BrdU, except for TRA-1-60 (+) cells on day 7 after OSKM induction, indicating that MYC contributed to the re-establishment of proliferation. To confirm whether MYC promotes proliferation of TRA-1-60 (+) cells rather than conversion to a TRA-1-60 (+) fate, we separated ESRG (+)/TRA-1-60 (+) or ESRG (+)/TRA-1-60 (–) cells on day 4 of reprogramming and analyzed the existence of TRA-1-60 (+) cells on day 7. Day 4 ESRG (+)/TRA-1-60 (–) cells produced few TRA-1-60 (+) cells by day 7 (Figures 2G and 2H), suggesting that MYC did not promote *de novo* conversion to a TRA-1-60 (+) state.

Initiation of ESRG (+) and TRA-1-60 (+) Fate Depends on Neither Proliferation nor MYC

The finding that early reprogramming cells stop proliferating prompted us to examine whether proliferation is required for emergence of ESRG (+) and TRA-1-60 (+) cells. To this end, we treated ESRG-Clover fibroblasts and HDFs with mitomycin C (MMC) to arrest their proliferation 1 day after OSK or OSKM transduction. Counting of treated cells over 7 days showed that MMC treatment resulted in negligible proliferation, without detectable BrdU labeling (Figures S2A and S2B). However, ESRG (+) cells were readily detected even from MMC-treated fibroblasts on day 3 post-transduction of OSK or OSKM (Figure 2I). The proportion of ESRG (+) cells in MMC-treated cells was comparable to that of untreated fibroblasts (Figure 2I). This was also the case with the proportion of TRA-1-60 (+) cells on day 4 (Figure 2J). On day 7, the proportion of TRA-1-60 (+) cells did not increase from day 4 in MMC-treated cells, whereas it increased significantly in OSKM-transduced, MMC-untreated cells (Figure 2J). Comparable results were observed with aphidicolin, a reversible inhibitor of eukaryotic nuclear DNA replication and cell-cycle progression (Figures S2C and S2D).

Next, we examined whether endogenous MYC was required for early reprogramming. Among the three MYC family members—MYC (also known as c-MYC), MYCN, and MYCL—we found that only MYC was expressed in fibroblasts (Figure 2K). Thus, we knocked down endogenous MYC using short hairpin RNA (shRNA) in OSK-induced reprogramming (Figure 2L). However, suppression of endogenous MYC did not alter the emergence of ESRG (+) cells on day 3 or TRA-1-60 (+) cells on day 4 (Figure 2M).

(J) MYC does not affect first emergence of TRA-1-60 (+) cells. Percentages of TRA-1-60 (+) cells from MMC-treated (+) or non-treated (–) HDFs on days 4 and 7 post-transduction of OSK or OSKM are shown. $n = 3$. See also Figure S2.

(K) Relative expression of MYC family genes c-MYC, MYCN, and MYCL compared to GAPDH expression in iPSCs and fibroblasts (Fib) analyzed by qRT-PCR. $n = 3$.

(L) Knockdown of c-MYC in fibroblasts. Shown is the expression of c-MYC in fibroblasts that were introduced with empty vector (Mock) or c-MYC shRNA analyzed by qRT-PCR. $n = 3$.

(M) Endogenous MYC does not affect the initiation of reprogramming. Shown are the percentages of ESRG (+) cells (green) on days 3 and 4 and TRA-1-60 (+) cells on day 4 induced by OSK with or without c-MYC shRNA. $n = 3$.

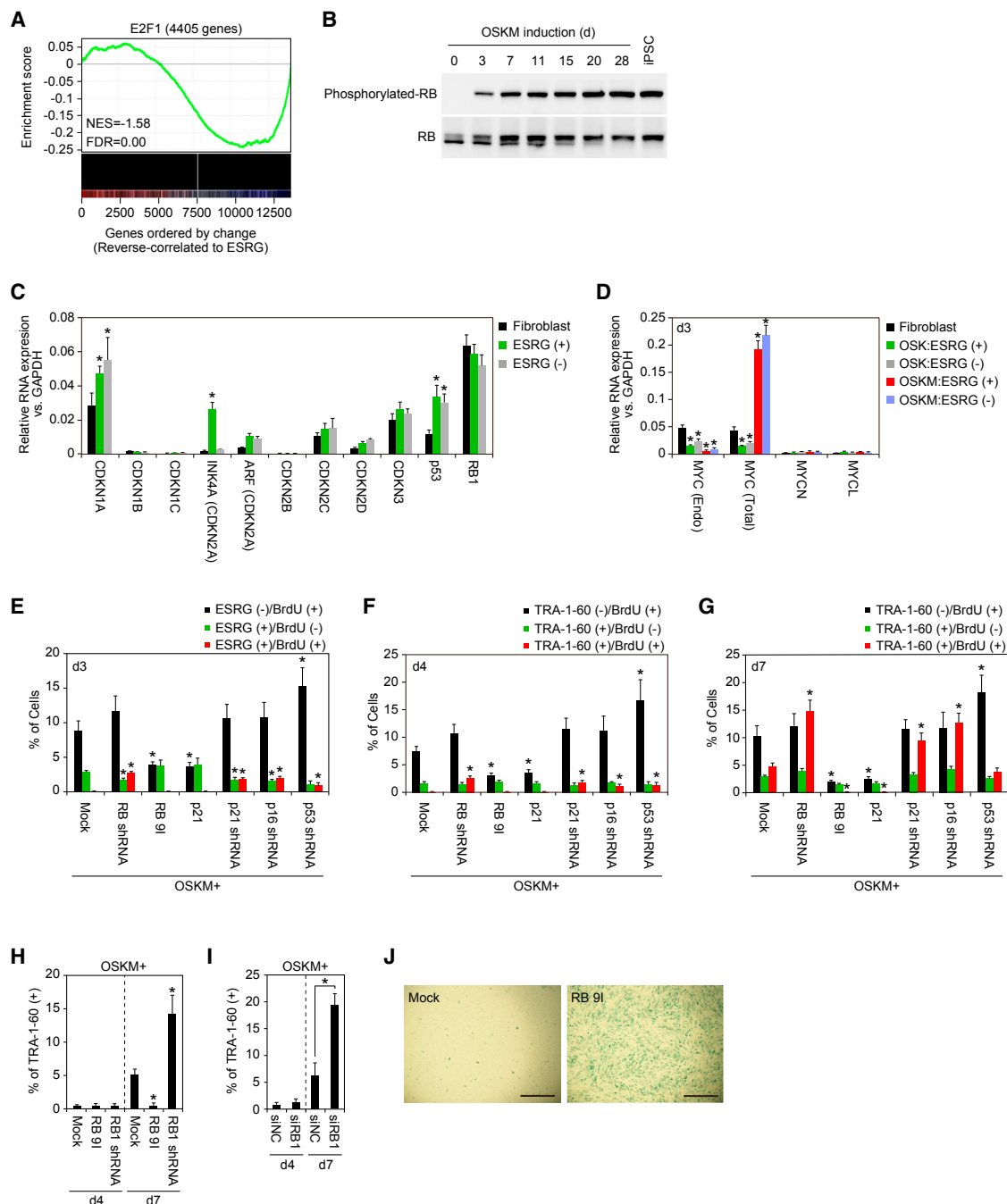


Figure 3. RB Activity Must Be Attenuated for TRA-1-60 (+) Cell Proliferation

(A) Gene set enrichment analysis plot showing enrichment of genes with binding of E2F1 at promoters (± 500 bp from the transcription start site) in the set of genes that show reverse correlation with ESRG expression. x axis shows genes ranked by the Pearson correlation coefficient for ESRG expression. Left, positively correlated genes; right, negatively correlated genes. See also [Figure S3](#) and [Tables S3](#) and [S4](#).

(B) Phosphorylation statuses of RB during reprogramming. Phosphorylated RBs (upper) and total RBs (lower) during reprogramming from HDFs to iPSCs induced by OSKM were detected by western blotting.

(C) Expression of CDK inhibitors in the early stages of reprogramming. Shown are relative expressions of genes encoding CDK inhibitor proteins in ESRG-Clover fibroblast, ESRG (+), or ESRG (-) cells on day 3 post-transduction of OSKM analyzed by qRT-PCR. * $p < 0.05$ versus fibroblasts by unpaired t test ($n = 3$). See also [Figure S4](#).

(D) OSK suppresses endogenous MYC expression. Shown is the relative expression of endogenous MYC, total MYC, MYCN, and MYCL compared to expression of GAPDH in ESRG (+) or ESRG (-) cells induced by OSK or OSKM on day 3. * $p < 0.05$ versus fibroblasts by unpaired t test ($n = 3$).

(legend continued on next page)

RB Activity Is Crucial for Proliferation Pause in Early Reprogramming Cells

To address mechanisms of the proliferation pause in early reprogramming cells, we analyzed single-cell RNA-seq data to determine whether genes that correlated with ESRG expression associated with a specific functional pathway or pathways (Table S4). We found that the RB/E2F pathway was highly associated with genes that inversely correlated with ESRG expression (Figures 3A and S3). Of 6,717 genes that inversely correlated with ESRG expression and 4,405 genes with promoter regions occupied by E2F1, 2,339 genes overlapped ($p < 2.2 \times 10^{-16}$ by Fisher's exact test) (Figure 3A). Consistently, western blot analyses demonstrated that phosphorylated RB, an inactive form of RB, increased as reprogramming progressed (Figure 3B). We also found that ESRG (+) cells on day 3 after OSK or OSKM transduction expressed high levels of CDKN1A and INK4A (Figures 3C and S4A). TP53 mRNA, which encodes the p53 tumor suppressor, was also induced by OSK or OSKM in ESRG (+) cells (Figures 3C and S4A). Increased p53 at least partly contributed to the increase of CDKN1A mRNA (el-Deiry et al., 1993). In addition, we found that OSK suppressed the expression of the endogenous MYC (Figure 3D). All of these changes should contribute to activation of RB (Muñoz-Espín and Serrano, 2014), sequestration of E2F, and decrease of proliferation.

To study the roles of RB1, p16, p21, and p53 in early reprogramming cells, we suppressed their expression using specific shRNAs. We found that inhibition of these tumor suppressor genes induced DNA synthesis in ESRG (+) cells on day 3 and TRA-1-60 (+) cells on day 4, as judged by BrdU incorporation (Figures 3E, 3F, S4B, and S4C). They also facilitated DNA synthesis of TRA-1-60 (+) cells on day 7 (Figures 3G and S4C). These data show that the three tumor suppressor gene products, p16, p21, and p53, cooperatively activate RB and suppress proliferation. Increased DNA synthesis resulting from RB1 shRNA treatment did not immediately increase the proportion of TRA-1-60 (+) cells on day 4, but it did significantly increase on day 7 after OSK or OSKM transduction (Figures 3H and S4E). We observed comparable results with transfection of small interfering RNA (siRNA) targeting RB1 (Figures 3I and S4F).

Forced expression of the constitutive active mutant of RB (RB 9l) or p21 strongly suppressed the proliferation of TRA-1-60 (+) cells on day 7 after OSKM induction (Figures 3E–3G).

As a consequence, activation of the RB pathway significantly reduced the proportion of TRA-1-60 (+) cells on day 7 after induction of OSKM, but not of OSK (Figures 3G, 3H, S4D, and S4E). After transduction of RB 9l, along with OSKM, many cells became positive for senescence-associated β -galactosidase (β -gal) (Figure 3J). They did not affect the emergence of ESRG (+) cells on day 3 and TRA-1-60 (+) cells on day 4 (Figures 3E, 3F, S4B, and S4C). These data suggest that RB does not interfere with the emergence of early reprogramming cells but does inhibit their proliferation and induce senescence.

MYC Activates LIN41, which Promotes RB Inactivation

To understand how exogenous MYC attenuates RB activity in early reprogramming cells, we selected 13 pluripotency-associated genes and transcription factor genes (Figure 4A) from the list of genes that were commonly upregulated during early reprogramming from five somatic cells (Figure 1A; Table S1). We examined whether forced expression of these 13 genes increased the proportion of TRA-1-60 (+) cells. We found that one of them, LIN41 (also known as TRIM71), significantly increased TRA-1-60 (+) cells on day 7 after OSKM transduction (Figure 4A). Although we previously showed that LIN41 enhanced human iPSC generation, its molecular mechanism or mechanisms remain unclear (Worringer et al., 2014).

Single-cell RNA-seq revealed that endogenous LIN41 expression was detected only in TRA-1-60 (+) cells (Figure 4B). Compared to the expression pattern of ESRG (Figure 1B), the expression of LIN41 on day 3 after OSKM transduction was lower. To confirm this, we examined the expression of LIN41 and ESRG in ESRG-Clover (+) cells on day 3 and TRA-1-60 (+) cells on day 7 after OSKM transduction (Figure 4C). We found that LIN41 expression remained low on day 3 but increased on day 7. Immunocytochemistry detected endogenous LIN41 proteins 7 days after transduction with OSKM, but not OSK (Figure 4D). However, both OSK and OSKM increased LIN41 mRNA to comparable levels on day 7 (Figure 4E). We also found that let-7 family miRNAs, which target LIN41 mRNA to inhibit translation, were suppressed by MYC (Figure 4F) (Chang et al., 2008). These data indicate that OSK induces LIN41 mRNA, but without MYC, LIN41 protein cannot be produced due to let-7.

Knockdown of endogenous LIN41 did not change the proportion of new TRA-1-60 (+) cells on day 4 but canceled

(E) RB pathway affects proliferation of ESRG (+) cells. Shown are the percentages of ESRG (–)/BrdU (+) cells (black), ESRG (+)/BrdU (–) cells (green), and ESRG (+)/BrdU (+) cells (red) on day 3 post-transduction of OSKM, along with each indicated factor to ESRG-Clover fibroblasts. * $p < 0.05$ versus Mock by unpaired t test ($n = 3$). See also Figure S4.

(F) RB pathway affects proliferation of new TRA-1-60 (+) cells. Shown are the percentages of TRA-1-60 (–)/BrdU (+) cells (black), TRA-1-60 (+)/BrdU (–) cells (green), and TRA-1-60 (+)/BrdU (+) cells (red) on day 4 post-transduction of OSKM, along with each indicated factor to HDFs. * $p < 0.05$ versus Mock by unpaired t test ($n = 3$). See also Figure S4.

(G) RB pathway affects proliferation of TRA-1-60 (+) cells. Shown are the percentages of TRA-1-60 (–)/BrdU (+) cells (black), TRA-1-60 (+)/BrdU (–) cells (green), and TRA-1-60 (+)/BrdU (+) cells (red) on day 7 post-transduction of OSKM, along with each indicated factor to HDFs. * $p < 0.05$ versus Mock by unpaired t test ($n = 3$). See also Figure S4.

(H) Effects of RB on early stage of reprogramming. The graph shows the relative proportion of TRA-1-60 (+) cells 7 days after transduction of OSKM, along with empty vector (Mock), RB 9l, or RB1 shRNA to HDFs. RB inactivation enhances the proportion of TRA-1-60 (+) cells. * $p < 0.05$ versus Mock by Dunnett's test ($n = 3$). See also Figure S4.

(I) Inactivation of RB facilitates expansion of early TRA-1-60 (+) cells. Shown are the effects of RB1 knockdown by siRNA transfection on the OSKM-induced TRA-1-60 (+) cell proportion on day 4 (d4) and day 7 (d7). * $p < 0.05$ by unpaired t test ($n = 3$). See also Figure S4.

(J) RB activity is associated with senescence in early phase of reprogramming. Representative images of HDFs 7 days after transduction of OSKM, along with empty vector (Mock) or RB 9l with staining for senescence-associated β -gal. Bars indicate 200 μ m.

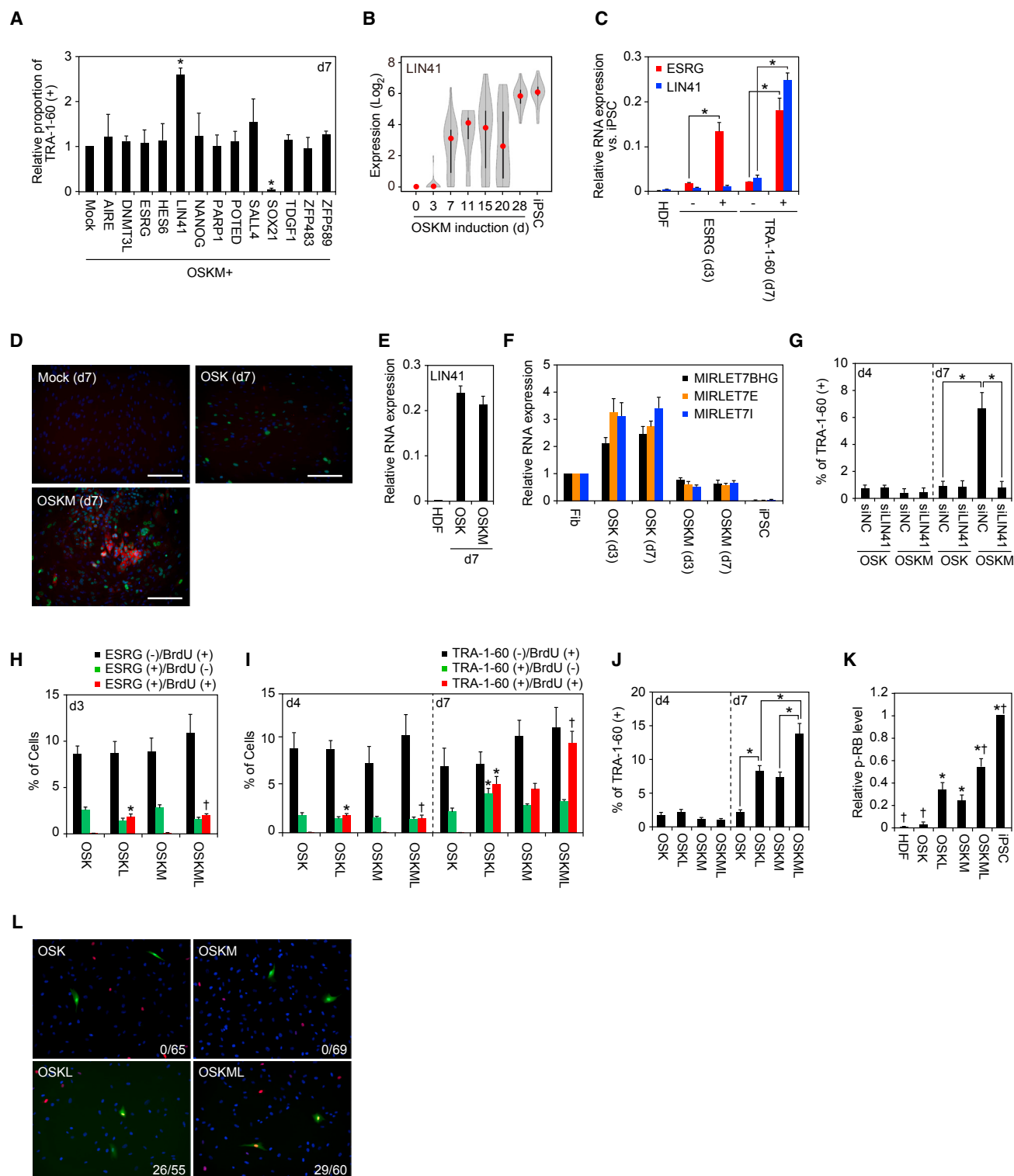


Figure 4. LIN41 Enhances Early Reprogramming Process with RB Inactivation

(A) LIN41 enhances the proportion of TRA-1-60 (+) cells from HDFs. Shown are relative proportions of TRA-1-60 (+) cells 7 days after transduction of OSKM, along with each indicated factor to HDFs. **p* < 0.05 by Dunnett's test (*n* = 3).

(B) LIN41 is activated in TRA-1-60 (+) cells during reprogramming. Shown is the expression of LIN41 during reprogramming from HDFs to iPSCs analyzed by single-cell RNA-seq. Twenty-four single cells were analyzed for each sample. Red dots indicate median values. Gray hourglass shapes represent the distribution of RPKM + 1 value.

(legend continued on next page)

MYC-induced expansion of TRA-1-60 (+) cells on day 7 (Figure 4G). In contrast, LIN41 knockdown did not affect the proportion of TRA-1-60 (+) cells induced by OSK on days 4 and 7 (Figure 4G), which was reasonable, because LIN41 protein was not expressed in these early reprogramming cells after OSK transduction. These data suggest that induction of LIN41 is responsible for the expansion of TRA-1-60 (+) cells by MYC.

We then examined the effect of exogenous LIN41 on early reprogramming cells. When transduced together with OSK or OSKM, LIN41 induced proliferation of ESRG (+) cells on day 3 (Figure 4H) and TRA-1-60 (+) cells on day 4 (Figure 4I), as judged by BrdU incorporation. This is in contrast to MYC, which did not induce DNA synthesis on days 3 and 4 when co-transduced with OSK. However, on day 7, both LIN41 and MYC promoted cell proliferation (Figure 4I) and increased the proportion (Figures 4J) of TRA-1-60 (+) cells. These data suggest that activation of LIN41 protein expression induced by MYC promotes the expansion of early TRA-1-60 (+) cells.

Next, to confirm whether LIN41 contributes to inactivation of RB activity, we checked the phosphorylation statuses of RB in HDFs transduced with OSK and OSKM with or without LIN41. We found that OSKM, but not OSK, caused the increase of phosphorylated RB in HDFs, albeit at a low efficiency (Figures 4K and S5). Exogenous LIN41 with either OSK or OSKM significantly increased phosphorylated RB (Figures 4K and S5). Furthermore, immunohistochemistry detected many ESRG (+) cells on day 3 that were positive for phosphorylated RB when exogenous LIN41 was added to OSK or OSKM (Figure 4L). In contrast, we did not detect phosphorylated RB in ESRG (+) cells without LIN41. Thus, LIN41 promotes phosphorylation of RB in early reprogramming cells.

LIN41 Suppresses p21 Protein Expression

To better understand how LIN41 contributes to RB inactivation, we searched for LIN41's target RNAs by immunoprecipitation of

endogenous LIN41 from human ESCs. We found that CDKN1A mRNA encoding p21 was the most highly enriched among LIN41-bound mRNAs (Figure 5A; Table S5). Other RB-related genes, including RB1 and INK4A, were not found as LIN41's targets. In TRA-1-60 (+) cells on day 7, exogenous LIN41 with OSK or OSKM significantly lowered the p21 protein level (Figure 5B). MYC induced LIN41 protein expression and lowered p21 protein levels, albeit with lower efficiency than exogenous LIN41 (Figure 5B).

We hypothesized that LIN41, which is an RNA-binding protein, regulates p21 protein levels rather than transcription in the early stage of reprogramming. In accordance with this hypothesis, LIN41 did not affect CDKN1A mRNA expression (Figure 5C). Immunocytochemistry of cultures on day 7 post-transduction of various combination of reprogramming factors, such as OSK; OCT3/4, SOX2, KLF4 and LIN41 (OSKL); OSKM; and OCT3/4, SOX2, KLF4, MYC and LIN41 (OSKML); showed a few in which LIN41 and p21 expression overlapped (Figure 5D). In addition, immunohistochemistry with anti-p21 antibody showed that forced expression of LIN41 alone in HDFs was sufficient to eliminate endogenous p21 proteins, although the CDKN1A mRNA level was not changed by LIN41 (Figures 5E–5G). These data suggest that CDKN1A mRNA is a direct target of LIN41 in human cells rather than an ESC-specific miRNA-dependent mechanism (Chang et al., 2012).

MYC Suppresses p16, Another Mechanism of RB Inactivation

In addition to LIN41-mediated p21 suppression, we found that MYC downregulated p16 expression, which was induced by OSK (Figure 5B). In contrast to the post-transcriptional regulation of p21 encoded by CDKN1A, MYC downregulated the RNA levels of INK4A in early reprogrammed cells (Figure 5C). LIN41 affected neither p16 protein nor INK4A mRNA levels (Figures 5B and 5C). These data suggest MYC suppressed RB

(C) LIN41 is silenced in ESRG (+) cells. Shown is the expression of ESRG and LIN41 in HDFs, ESRG (+) cells, or ESRG (–) cells on day 3 and TRA-1-60 (+) or TRA-1-60 (–) cells on day 7 analyzed by qRT-PCR. * $p < 0.05$ by unpaired t test ($n = 3$).

(D) OSKM induces LIN41 protein expression in early stage of reprogramming. Panels show the immunocytochemistry of HDFs transduced with empty vector (Mock, upper left), OSK (upper right), or OSKM (lower left) with LIN41 (red) and OCT3/4 (green) antibodies. Nuclei were visualized by Hoechst 33342 staining. Bars indicate 100 μm .

(E) MYC does not affect LIN41 mRNA expression. Shown is the relative expression of LIN41 transcript in TRA-1-60 (+) cells induced by OSK or OSKM on day 7, compared to Mock. $n = 3$.

(F) MYC suppresses OSK-induced let-7 expression. Shown is the relative expression of MIRLET7BHG, MIRLET7E, and MIRLET7I pre-miRNAs in ESRG (+) cells on day 3 and TRA-1-60 (+) cells on day 7 induced by OSK or OSKM, compared to those in fibroblasts (Fib). * $p < 0.05$ versus fibroblast by unpaired t test ($n = 3$).

(G) LIN41 is required for efficient reprogramming in the early phase. Shown are the effects of LIN41 knockdown by siRNA transfection on OSK- or OSKM-induced TRA-1-60 (+) cell proportion on day 4 (d4) and day 7 (d7). * $p < 0.05$ by unpaired t test ($n = 3$).

(H) LIN41 affects proliferation of ESRG (+) cells. Shown are the percentages of ESRG (–)/BrdU (+) cells (black), ESRG (+)/BrdU (–) cells (green), and ESRG (+)/BrdU (+) cells (red) on day 3 post-transduction of OSK or OSKM, along with empty vector (Mock) or LIN41 to ESRG-Clover fibroblasts. * $p < 0.05$ versus OSK and † $p < 0.05$ versus OSKM by unpaired t test ($n = 3$). OSKM data are identical to Mock in Figure 3E.

(I) LIN41 affects proliferation of TRA-1-60 (+) cells. Shown are the percentages of TRA-1-60 (–)/BrdU (+) cells (black), TRA-1-60 (+)/BrdU (–) cells (green), and TRA-1-60 (+)/BrdU (+) cells (red) on day 4 and day 7 post-transduction of OSK or OSKM, along with empty vector (Mock) or LIN41 to HDFs. * $p < 0.05$ versus OSK and † $p < 0.05$ versus OSKM by unpaired t test ($n = 3$). OSKM data are identical to Mock in Figures 3F and 3G.

(J) LIN41 facilitates expansion of early TRA-1-60 (+) cells. Shown are the effects of LIN41 overexpression on OSK- or OSKM-induced TRA-1-60 (+) cell proportion on day 4 (d4) and day 7 (d7). * $p < 0.05$ by unpaired t test ($n = 3$).

(K) LIN41 increases phosphorylation states of RB. Shown are the relative intensities of phosphorylated RB in HDFs, iPSCs, and HDFs expressing OSK, OSKL, OSKM, or OSKML on day 4 by western blotting. * $p < 0.05$ versus OSK and † $p < 0.05$ versus OSKM by t test ($n = 3$). See also Figure S5.

(L) Status of phosphorylated RB in ESRG (+) cells. Shown are representative images of ESRG (+) cells (green) after 3 days of OSK, OSKL, OSKM, or OSKML transduction stained with phosphorylated RB (red) antibody. Nuclei (blue) were visualized by Hoechst 33342 staining. The indicated number at the lower-right corner of each panel is phosphorylated RB (+)/ESRG (+) cells.

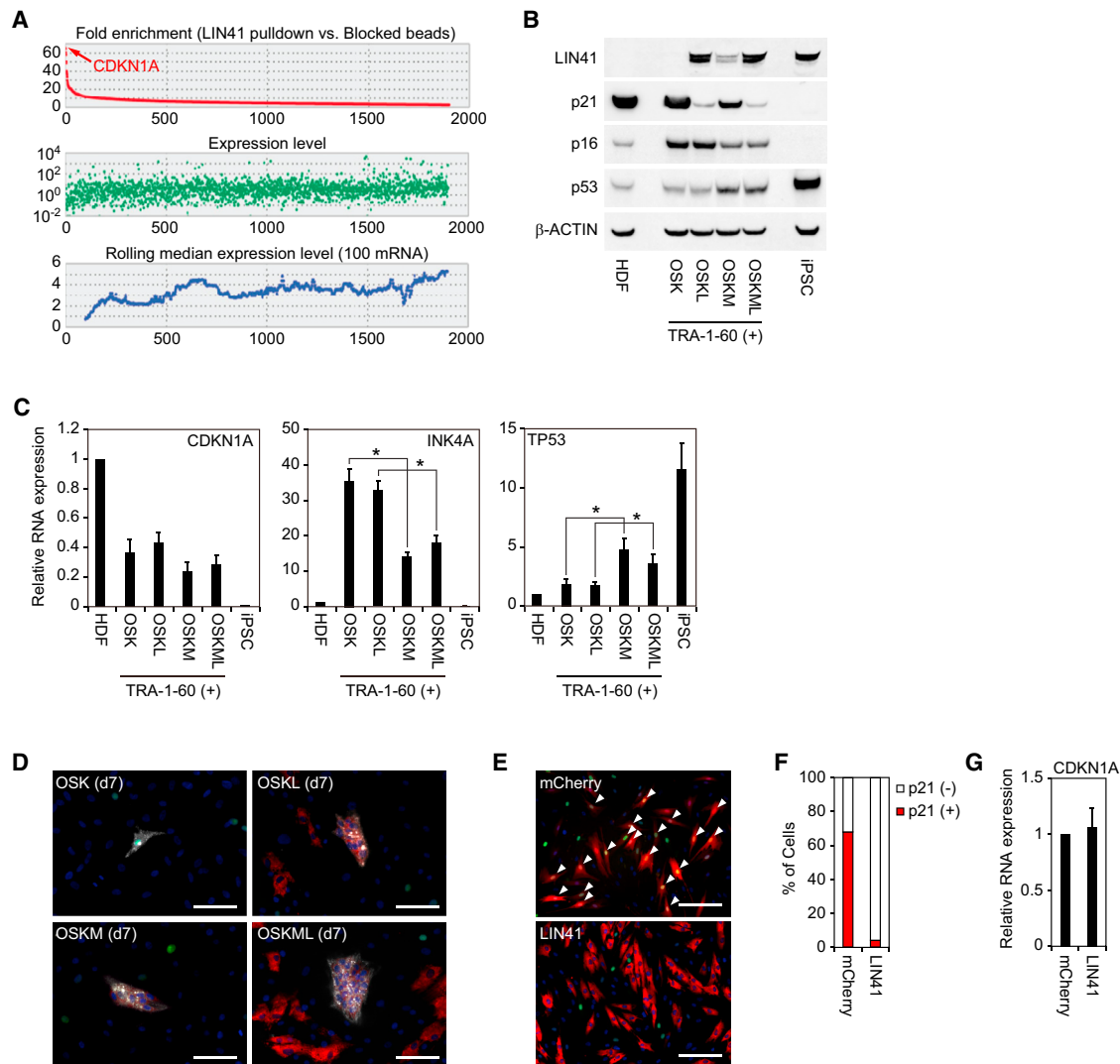


Figure 5. LIN41 Post-transcriptionally Suppresses p21

(A) LIN41-interacting RNAs. Upper panel shows fold enrichment of precipitated RNAs by LIN41 pull-down compared to those by beads blocked with LIN41 peptides. In addition, RNA expression levels (middle) and rolling median expression levels (lower) are shown. $n = 3$. See also Table S5.

(B) Western blot showing expression of LIN41, p21, p16, p53, and β -ACTIN proteins in HDFs; in TRA-1-60 (+) cells on day 7 post-transduction of OSK, OSKL, OSKM, or OSKML; and in iPSCs.

(C) Expression of CDKN1A, INK4A, and TP53 mRNAs in TRA-1-60 (+) cells on day 7 analyzed by qRT-PCR. * $p < 0.05$ by unpaired t test ($n = 3$).

(D) Representative immunocytochemistry images of TRA-1-60 (+) cells on day 7 post-transduction of OSK, OSKL, OSKM, or OSKML stained with TRA-1-60 (white), LIN41 (red), and p21 (green) antibodies. Nuclei were visualized using Hoechst 33342 (blue). Bars indicate 25 μ m.

(E) LIN41 suppresses p21 protein expression in reprogramming intermediates. Shown are representative images of immunocytochemistry of p21 (green) in HDFs expressing mCherry (red in left) or LIN41 (red in right). Nuclei were visualized using Hoechst 33342 (blue). Bars indicate 100 μ m. White arrowheads indicate the cells that express both transgene and p21.

(F) LIN41 suppresses the expression of p21 protein. The graph shows the quantitative results of (E). $n = 50$.

(G) LIN41 does not alter the expression of CDKN1A mRNA. Shown are relative expression of CDKN1A in HDFs expressing mCherry or LIN41. $n = 3$.

activity via dual inhibition of p16 and p21 by different modes of actions.

Immortalization Bypasses the Proliferation Pause

We found that a fibroblast line established from an iPSC-derived teratoma (TdFs) is different from HDFs in that the efficiency of iPSC generation by OSK alone was significantly higher (Fig-

ure 6A). MYC did not further increase OSK-mediated iPSC generation from TdFs (Figure 6B). The MYC-independency of TdFs gave us an unprecedented opportunity to elucidate roles of MYC in promoting OSK-mediated reprogramming from non-immortalized cells.

We found that even in TdFs, the proportion of TRA-1-60 (+) cells at day 4 was low (~2%) and comparable to that of HDFs

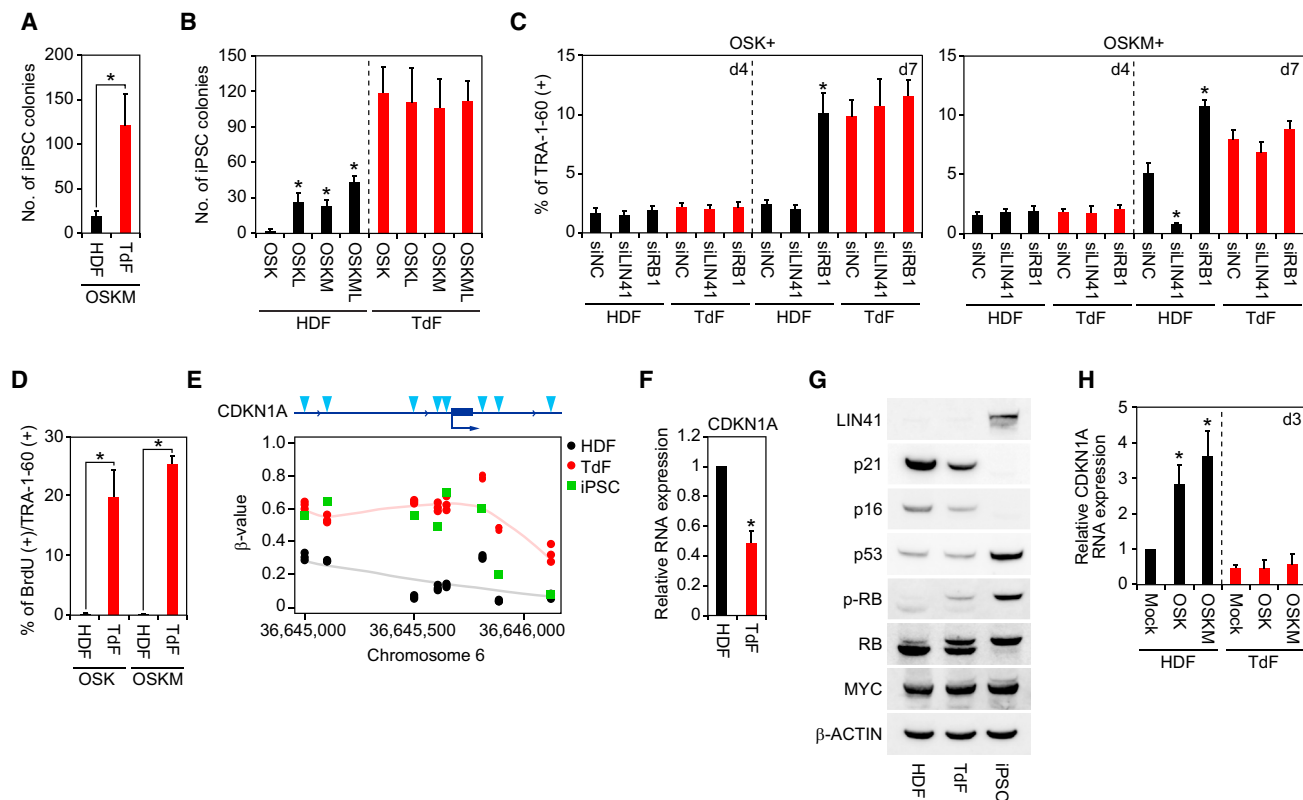


Figure 6. Immortalization Bypasses the Proliferation Pause

(A) Number of iPSC colonies on day 24 derived from 5×10^4 cells of OSKM-transduced HDFs and TdFs. *p < 0.05 by unpaired t test (n = 3).
 (B) Effects of exogenous MYC and LIN41 on iPSC generation from HDFs or TdFs. Shown are the number of iPSC colonies from HDFs or TdFs on day 24 post-transduction of OSK, OSKL, OSKM, or OSKML. *p < 0.05 by Dunnett's test (n = 3).
 (C) Effects of LIN41 or RB1 knockdown by siRNA transfection on the OSK- or OSKM-induced TRA-1-60(+) cell proportion from HDFs or TdFs on days 4 and 7. *p < 0.05 by Dunnett's test (n = 3).
 (D) Percentage of BrdU incorporation of newly converted TRA-1-60(+) cells from HDFs or TdFs on day 4 post-transduction of OSK or OSKM. *p < 0.05 by unpaired t test (n = 3).
 (E) DNA methylation status in the upstream region of the CDKN1A gene. Shown are the β value of DNA methylation at each CpG site (blue arrowheads) in the upstream region of the CDKN1A gene in HDFs (black), TdFs (red), and iPSCs (green) analyzed by Infinium. n = 3.
 (F) Relative expression of CDKN1A in HDFs and TdFs analyzed by qRT-PCR. *p < 0.05 versus HDFs by unpaired t test (n = 3).
 (G) Western blot showing expression of cell-cycle-related proteins LIN41, p21, p16, p53, MYC, and β -actin proteins in HDFs, TdFs, and iPSCs.
 (H) No induction of CDKN1A by OSKM in TdFs. Shown is the relative expression of CDKN1A mRNA in HDFs (black) or TdFs (red) on day 3 post-transduction of empty vector (Mock), OSK, or OSKM. *p < 0.05 by Dunnett's test (n = 3).

(Figure 6C). This showed that the initial appearance of reprogramming cells is not responsible for the high reprogramming efficiency of TdFs. However, ~20% of TRA-1-60(+) cells from TdFs showed BrdU incorporation on day 4 after OSK or OSKM (Figure 6D). This resulted in a significant increase of TdF-derived TRA-1-60(+) cells to ~10% on day 7 (Figure 6C). Inhibiting endogenous LIN41 or RB1 did not affect the proportion of TdF-derived TRA-1-60(+) cells on day 7 (Figure 6C). These data showed that TdFs do not require MYC to overcome an RB-mediated proliferation pause in early reprogramming cells.

To clarify why TdFs bypass the proliferation pause, we analyzed DNA methylation and gene expression in HDFs and TdFs. CpG sites in the upstream region of the CDKN1A gene in TdFs and in iPSCs were hyper-methylated compared to those in HDFs (Figure 6E). In parallel, expression of CDKN1A mRNA and p21 protein in TdFs was significantly lower than in HDFs

(Figures 6F and 6G). Furthermore, OSK or OSKM transduction significantly increased CDKN1A expression on day 3 in HDFs, but not in TdFs (Figure 6H). We also detected lower p16 and higher phosphorylated RB expression in TdFs than in HDFs (Figure 6G). However, c-MYC and p53 protein expression in TdFs was comparable to those in HDFs (Figure 6G). In addition, TdFs were resistant to premature senescence induced by forced expression of constitutive active mutant of HRas (HRasV12, mutated Gly12 to Val) or RB 9I (Figures S6A and S6B). These data demonstrated that constitutive inactivation of p21, p16, and RB in TdFs contributes to MYC independency.

We next used TdFs to examine other MYC functions that had been reported as mechanisms to promote reprogramming, including changing metabolisms (Folmes et al., 2013), facilitating OSK binding to their targets (Soufi et al., 2012), and suppressing fibroblast-specific genes (Li et al., 2010; Nakagawa et al., 2010).

We cultured HDFs, TdFs, and iPSCs in culture media containing 2-deoxy-D-glucose (2-DG), a potent blocker of glycolytic metabolism (Woodward and Hudson, 1954). In this condition, iPSCs did not survive, because they largely depend on glycolytic metabolism (Figure S6C). In contrast, both HDFs and TdFs proliferated normally. In addition, we examined expression levels of oxidative phosphorylation markers (e.g., ACO1, IDH2, MDH1, and SDHD) and glycolysis markers (e.g., ENO3, PYGM, SLC16A1, and SLC2A4) (Varum et al., 2011) by qRT-PCR. We found that TdFs and HDFs share similar expression patterns, indicative of oxidative metabolism (Figure S6D). Thus, it is unlikely that metabolic effects of MYC play a major role in promoting iPSC generation.

We next examined whether OSK binding sites are more accessible in TdFs than in HDFs. To this end, we analyzed DNA methylation signatures of CpG islands of OSK binding sites (Figure S6E). We found no evidence that these sites were open, as characterized by lower DNA methylation. TdFs showed slightly but significantly higher DNA methylation for all three transcription factors: OSK. In addition, the expression levels of OSK-binding genes were comparable in TdFs and HDFs (Figure S6F). Thus, increase in OSK binding is not responsible for the high reprogramming efficiency of TdFs.

Finally, we examined the expression levels of fibroblast-specific genes. We selected 2,449 genes whose expression levels were at least 5-fold higher in HDFs than in iPSCs. RNA-seq analyses showed that the expression levels of these genes were significantly lower in TdFs than in HDFs but still higher than in iPSCs (Figure S6G). This result suggests that the suppression of fibroblast-specific genes may also contribute to the high reprogramming efficiency of TdFs.

DISCUSSION

MYC affects several important biological processes through DNA binding and subsequent transcriptional activation or inhibition of a diverse set of target genes. To define MYC's role in reprogramming, previous reports compared OSK to OSKM reprogramming and found several MYC-dependent correlations. These include enhancement or alteration of OSK binding, promotion of ESC-like metabolic changes, and enhancement of proliferation (Chappell and Dalton, 2013; Soufi et al., 2012; Sridharan et al., 2009). Each of these observed changes may or may not play a major role in the outcome of reprogramming (enhanced colony formation), and we are cognizant of the gap between correlation and causation in this complicated system. To specifically address the significance of a particular function of a multifunctional protein, we need to isolate that particular function and determine its importance. Mutating MYC to isolate a specific biological process (chromatin accessibility versus metabolism versus proliferation) is not feasible: varied biological pathways depend on this transcription factor. In this work, we identified two methods for replacing one particular aspect—enhancement of proliferation—of MYC. This enabled us to weigh MYC's contribution to proliferation in reprogramming. Both of these methods are discussed in detail here.

In addition to the strategies for replacing MYC, identification of ESRG as an early maker of reprogramming proved useful,

because it allowed us to precisely define cellular and molecular events during the first few days after OSK or OSKM induction. Our data demonstrate that OSK elicits two important molecular events in human cells: the initiation of the reprogramming process and the RB-mediated proliferation pause or blockade. MYC does not affect the first event, but it promotes iPSC generation by escaping the proliferation pause.

The first molecular event that OSK elicits is initiation of the reprogramming process, including activating early markers such as ESRG and TRA-1-60. We and others report that activation of endogenous retroviruses is crucial for iPSC generation in human cells. ESRG is a lncRNA driven by long terminal repeat (LTR) 7 of a HERV-H group endogenous retrovirus (Li et al., 2013; Lu et al., 2014; Ohnuki et al., 2014; Wang et al., 2014). We found that the LTR7 of ESRG contains the binding site of KLF4, suggesting that OSK directly activates its expression (Ohnuki et al., 2014). To our surprise, MYC did not promote this initial process of reprogramming. This is in contrast to a previous report that MYC enhanced the binding of OSK to its targets. Furthermore, we found that even endogenous MYC seemed dispensable for the appearance of ESRG (+) cells. Thus, MYC does not play a crucial role in this early event during human iPSC generation.

The other molecular event that OSK elicits is the proliferation pause in early reprogramming cells. Few BrdU (+) cells were detected in ESRG (+) cells on day 3 and TRA-1-60 (+) cells on day 4 after induction of OSK. We found that the OSK-mediated proliferation pause was attributable to RB activation. We also found that OSK induced expression of p16 and p53. OSK also induced a transient increase in p21 mRNA levels on day 3. Suppression of these genes by shRNAs induced proliferation. Thus, cooperation of these multiple tumor suppressor gene products is responsible for RB activation and the proliferation pause in early reprogramming cells. Previously, evidence of an oncogene-induced, senescence-like process was detected via transcriptional changes and described as reprogramming-induced senescence (Banito et al., 2009; Utikal et al., 2009). In this paper, we refer to the period from day 3 to day 7 as a proliferation pause or blockade, but we have no objection to alternatively calling the OSK-initiated, p21/p16-driven cessation of proliferation a reprogramming-induced senescence. We think the two processes are likely the same. With regards to this process, this work demonstrates the utility of ESRG to define the precise timing and demonstrates the mechanisms by which reprogramming cells are able to overcome this blockade.

MYC provided an escape from the proliferation pause elicited by OSK in early reprogramming cells. An important mechanism is the let-7/LIN41/p21 axis. OSK increased transcripts of let-7 family members, but addition of MYC suppressed this increase. We found that LIN41 mRNA expression was induced by OSK in early reprogramming cells. However, the LIN41 protein level remained low due to the increased expression of let-7 that inhibits translation of LIN41 mRNA (Lin et al., 2007; Slack et al., 2000). MYC, by suppressing let-7 expression, increases LIN41 protein. We also found that CDKN1A mRNA encoding p21 is the most enriched mRNA binding target in LIN41 pull-down from human ESCs (Figure 5A). Furthermore, LIN41 expression in fibroblasts dramatically represses p21 translation (Figure 5E). Thus, MYC

decreased p21 protein expression, leading to inactivation of RB and initiation of proliferation.

Though less dramatic than the effects on the let-7/LIN41/p21 axis, we additionally found that MYC decreased mRNA and protein levels of p16. When MYC alone is overexpressed, it induces p16 expression (Guney et al., 2006), but when it is co-expressed with RAS, MYC suppresses RAS-induced senescence (Hydbring et al., 2010). We suspect that a similar mechanism operates during reprogramming. In contrast to p16, MYC increased mRNA expression of p53, which should have an inhibitory influence on reprogramming (Figure 5C). We suppose that the suppression of p21 and p16 is sufficient to overcome negative effects of increased p53.

Because a proliferation pause was commonly observed in early reprogramming cells derived from five types of somatic cells, it might be a required step for reprogramming. However, TdFs reprogram without going through a proliferation pause. Furthermore, addition of exogenous LIN41 with OSK allows even somatic cells to avoid the onset of the proliferation pause. Therefore, a proliferation pause is not required in reprogramming; instead, it is a barrier to reprogramming that is common to normal somatic cells (five of five lines) when induced with OSK.

TdFs gave us a unique opportunity to delineate the roles of MYC in promoting reprogramming. TdFs were highly efficient in iPSC generation, and MYC did not enhance reprogramming. This suggests that the main role or roles of MYC are already achieved in TdFs. We found that an RB-mediated proliferation pause does not occur in TdFs even without exogenous MYC. OSK and OSKM reprogramming efficiencies were equal (Figure 6B). In contrast, we did not observe metabolic changes in favor of reprogramming in TdFs (Figure S6C). Our data also suggested that the binding of OSK to their target was comparable between TdFs and HDFs (Figures S6E and S6F). We did observe a significant downregulation of fibroblast-specific genes in TdFs compared to HDFs, suggesting that this intermediate level of expression may contribute to high reprogramming efficiency of TdFs (Figure S6G). However, given that TdFs have an intermediate level of HDF markers, further downregulation of many fibroblast-related genes and upregulation of many ESC-related genes are necessary to form iPSCs. If the previously proposed chromatin accessibility role of MYC significantly affected reprogramming efficiency, we would expect that TdFs would show a partial improvement upon addition of MYC. In addition, we would expect that the emergence of early reprogramming cells should be increased regardless of whether the downregulation of the fibroblast genetic program offered an easier route to reprogramming. Neither of these predictions (depending on a significant role for chromatin remodeling by MYC in reprogramming) is true in TdFs. Because proliferation pause-resistant TdFs do not benefit from MYC, we conclude that the main contribution of MYC in proliferation pause-responsive somatic cells is to overcome proliferation pause rather than to improve reprogramming through other means, such as chromatin accessibility.

We previously showed that LIN41, a cytoplasmic protein and a let-7 miRNA translationally repressed target, dramatically enhanced iPSC generation (Worringer et al., 2014). We identified EGR1, a transcription factor involved in differentiation, as a

target of LIN41. We showed that EGR1 protein was upregulated by LIN41 knockdown and LIN41 overexpression suppressed iPSC generation. Based on these data, we hypothesized that positive action of LIN41 in reprogramming is attributable to suppression of EGR1. However, our current results clearly show that p21 is the most crucial target of LIN41 in promoting iPSC generation. LIN41 enhances the reprogramming of OSK to the same extent as MYC (Figure 6B, see the right side of the HDF section). This is not coincidental, because LIN41 and MYC provide similar outcomes with regard to proliferation pause. OSKL reprogrammed cells subverted the proliferation pause by early and tight translational suppression of p21. OSKM entered the proliferation pause but eventually escaped after downregulation of let-7 miRNA, followed by derepression of endogenous LIN41 protein and subsequently p21 translational silencing. Again, LIN41 likely replaced only one specific biological function out of the various proposed mechanisms of MYC, but it achieved all of MYC's reprogramming enhancement. We therefore conclude that the significant contribution of MYC is that shared with LIN41—the ability to overcome proliferation pause.

We believe that the metabolic effects described as contingent upon MYC could be viewed as secondary to escape from the proliferation pause. In other words, when OSK is compared to OSKM, one is comparing blocked cells to cells that have escaped proliferation pause, continue to reprogram, and thus are continuing to gain ESC-like attributes (e.g., ESC-like metabolism). Regardless of whether a metabolic contribution is provided by MYC through transcriptional activation of metabolic genes or as a consequence of escape from the proliferation blockade, we find that an equivalent outcome is obtained by two methods that likely replace only MYC's effect on proliferation. Therefore, we favor a model emphasizing MYC's contribution as facilitating escape from a proliferation pause.

In conclusion, our data showed that the main function of MYC during human iPSC generation is to override an RB-mediated proliferation pause in early reprogramming cells. MYC achieves this by suppressing let-7 miRNA and derepressing endogenous LIN41 transcript. This leads to LIN41 protein-dependent translational repression of p21. Exogenous LIN41 fulfills the role of endogenous LIN41 and therefore MYC. In TdFs, the proliferation pause does not operate during reprogramming, resulting in MYC-independent high efficiency of iPSC generation. However, the emergence of early reprogramming cells is inefficient even with MYC or in TdFs. Therefore, the RB pathway is responsible for the proliferation pause, but not the low efficiency of the appearance of early reprogramming cells. Understanding the cause of the low conversion efficiency to the state demarcated by ESRG positivity—an early prerequisite for, but not a guarantee of, inevitable reprogramming—remains an important future task.

EXPERIMENTAL PROCEDURES

Further details and an outline of resources used in this work can be found in the [Supplemental Experimental Procedures](#).

Quantification and Statistical Analysis

Data are presented as mean \pm SD. Sample number (n) indicates the number of biological replicates in each experiment. The number of experimental repeats

is indicated in figure legends. To determine statistical significance, we used Dunnett's test for one-to-many comparisons and unpaired t test for comparisons between two groups using Excel 2013 (Microsoft) and Kaleida graph software (HULINKS) unless otherwise noted. Statistical significance in the main figures was set at $p < 0.05$, as indicated by an asterisk.

DATA AND SOFTWARE AVAILABILITY

The accession numbers for the gene expression microarray, Infinium, and deep sequencing results reported in this paper are GEO: GSE89455 and GSE90015. Raw images are accessible at the Mendeley website (<https://data.mendeley.com/datasets/wh59xb6sz6/draft?a=7db44554-6446-4c66-babe-d2080c43f0a1>).

SUPPLEMENTAL INFORMATION

Supplemental Information includes Supplemental Experimental Procedures, six figures, and six tables and can be found with this article online at <https://doi.org/10.1016/j.celrep.2018.03.057>.

ACKNOWLEDGMENTS

We thank A. Hotta, T. Kitamura, H. Niwa, K. Okita, H. Suemori, and J. Wang for providing materials; B. Conklin, M. Ohnuki, and K. Tomoda for discussions; and S. Arai, T. Hookway, Y. Inoue, K. Kaneko, T. Kato, J. Kuwahara, M. Lancero, Y. Nomiya, Y. Sawamura, I. Teramoto, M. Umekage, and the Gladstone Core Facilities of Stem Cell, Genomics, Flow Cytometry for technical assistance. We are also grateful to K. Essex, R. Fujiwara, H. Imagawa, R. Kato, E. Minamitani, Y. Miyake, S. Takeshima, and Y. Uematsu for administrative support and G. Howard for editorial assistance. This work was supported by Grants-in-Aid for Scientific Research from the Japanese Society for the Promotion of Science (JSPS) and from the Ministry of Education, Culture, Sports, Science, and Technology (MEXT); a grant from the Funding Program for World-Leading Innovative Research and Development in Science and Technology (First Program) of the JSPS; a grant from Core Center for iPS Cell Research, Research Center Network for Realization of Regenerative Medicine, MEXT; a grant from Japan Foundation for Applied Enzymology; and the iPS Cell Research Fund. The study was also supported by funding from Hiroshi Mikitani, Marc Benioff, the L.K. Whittier Foundation, the Roddenberry Foundation, the Gladstone Institutes, and NHLBI/NIH (U01-HL100406 and U01-HL098179). The Gladstone Institutes received support from a National Center for Research Resources grant (RR18928-01).

AUTHOR CONTRIBUTIONS

T.R., K.S., K. Tanabe, and K. Takahashi performed and analyzed most of the experiments with help from D.J. (flow cytometry). F.K. performed DNA methylation analyses. E.T. performed cell culture and DNA work, M. Narita performed RNA works such as microarrays and qPCR, and Michiko Nakamura performed flow cytometry and cell culture. M. Nomura, Masahiro Nakamura, and A.W. performed sample preparation and bioinformatic analyses. E.R., K. Tanabe, and K. Takahashi discussed and interpreted the analyses. S.Y. and K. Takahashi designed and directed research and wrote the manuscript, with editing by all authors.

DECLARATION OF INTERESTS

K.S. is employed by I Peace, Inc. K. Tanabe is a founder of I Peace, Inc. S.Y. is a scientific adviser (without salary) of iPS Academia Japan. K. Takahashi is on the scientific advisory board of I Peace, Inc. (without salary).

Received: May 16, 2017

Revised: February 14, 2018

Accepted: March 14, 2018

Published: April 10, 2018

REFERENCES

- Banito, A., Rashid, S.T., Acosta, J.C., Li, S., Pereira, C.F., Geti, I., Pinho, S., Silva, J.C., Azuara, V., Walsh, M., et al. (2009). Senescence impairs successful reprogramming to pluripotent stem cells. *Genes Dev.* 23, 2134–2139.
- Blackwell, T.K., Kretzner, L., Blackwood, E.M., Eisenman, R.N., and Weintraub, H. (1990). Sequence-specific DNA binding by the c-Myc protein. *Science* 250, 1149–1151.
- Blackwood, E.M., and Eisenman, R.N. (1991). Max: a helix-loop-helix zipper protein that forms a sequence-specific DNA-binding complex with Myc. *Science* 251, 1211–1217.
- Buganim, Y., Faddah, D.A., Cheng, A.W., Itskovich, E., Markoulaki, S., Ganz, K., Klemm, S.L., van Oudenaarden, A., and Jaenisch, R. (2012). Single-cell expression analyses during cellular reprogramming reveal an early stochastic and a late hierarchic phase. *Cell* 150, 1209–1222.
- Buganim, Y., Faddah, D.A., and Jaenisch, R. (2013). Mechanisms and models of somatic cell reprogramming. *Nat. Rev. Genet.* 14, 427–439.
- Chang, T.C., Yu, D., Lee, Y.S., Wentzel, E.A., Arking, D.E., West, K.M., Dang, C.V., Thomas-Tikhonenko, A., and Mendell, J.T. (2008). Widespread micro-RNA repression by Myc contributes to tumorigenesis. *Nat. Genet.* 40, 43–50.
- Chang, H.M., Martinez, N.J., Thornton, J.E., Hagan, J.P., Nguyen, K.D., and Gregory, R.I. (2012). Trim71 cooperates with microRNAs to repress Cdkn1a expression and promote embryonic stem cell proliferation. *Nat. Commun.* 3, 923.
- Chappell, J., and Dalton, S. (2013). Roles for MYC in the establishment and maintenance of pluripotency. *Cold Spring Harb. Perspect. Med.* 3, a014381.
- Chappell, J., Sun, Y., Singh, A., and Dalton, S. (2013). MYC/MAX control ERK signaling and pluripotency by regulation of dual-specificity phosphatases 2 and 7. *Genes Dev.* 27, 725–733.
- Ciriello, G., Miller, M.L., Aksoy, B.A., Senbabaoglu, Y., Schultz, N., and Sander, C. (2013). Emerging landscape of oncogenic signatures across human cancers. *Nat. Genet.* 45, 1127–1133.
- Cliff, T.S., Wu, T., Boward, B.R., Yin, A., Yin, H., Glushka, J.N., Prestegard, J.H., and Dalton, S. (2017). MYC Controls Human Pluripotent Stem Cell Fate Decisions through Regulation of Metabolic Flux. *Cell Stem Cell* 21, 502–516.
- Dang, C.V. (2012). MYC on the path to cancer. *Cell* 149, 22–35.
- Dang, C.V. (2013). MYC, metabolism, cell growth, and tumorigenesis. *Cold Spring Harb. Perspect. Med.* 3, a014217.
- Dang, C.V. (2015). Web of the extended Myc network captures metabolism for tumorigenesis. *Cancer Cell* 27, 160–162.
- Dominguez-Sola, D., and Gautier, J. (2014). MYC and the control of DNA replication. *Cold Spring Harb. Perspect. Med.* 4, a014423.
- el-Deiry, W.S., Tokino, T., Velculescu, V.E., Levy, D.B., Parsons, R., Trent, J.M., Lin, D., Mercer, W.E., Kinzler, K.W., and Vogelstein, B. (1993). WAF1, a potential mediator of p53 tumor suppression. *Cell* 75, 817–825.
- Fagnocchi, L., Cherubini, A., Hatsuda, H., Fasciani, A., Mazzoleni, S., Poli, V., Berno, V., Rossi, R.L., Reinbold, R., Ende, M., et al. (2016). A Myc-driven self-reinforcing regulatory network maintains mouse embryonic stem cell identity. *Nat. Commun.* 7, 11903.
- Folmes, C.D., Martinez-Fernandez, A., Faustino, R.S., Yamada, S., Perez-Terzic, C., Nelson, T.J., and Terzic, A. (2013). Nuclear reprogramming with c-Myc potentiates glycolytic capacity of derived induced pluripotent stem cells. *J. Cardiovasc. Transl. Res.* 6, 10–21.
- Gabay, M., Li, Y., and Felsher, D.W. (2014). MYC activation is a hallmark of cancer initiation and maintenance. *Cold Spring Harb. Perspect. Med.* 4, a014241.
- Guney, I., Wu, S., and Sedivy, J.M. (2006). Reduced c-Myc signaling triggers telomere-independent senescence by regulating Bmi-1 and p16(INK4a). *Proc. Natl. Acad. Sci. USA* 103, 3645–3650.
- Haupt, Y., Alexander, W.S., Barri, G., Klinken, S.P., and Adams, J.M. (1991). Novel zinc finger gene implicated as myc collaborator by retrovirally accelerated lymphomagenesis in E mu-myc transgenic mice. *Cell* 65, 753–763.

- Hayward, W.S., Neel, B.G., and Astrin, S.M. (1981). Activation of a cellular oncogene by promoter insertion in ALV-induced lymphoid leukosis. *Nature* 290, 475–480.
- Hydbring, P., Bahram, F., Su, Y., Tronnorsjö, S., Höglstrand, K., von der Lehr, N., Sharifi, H.R., Lilischkis, R., Hein, N., Wu, S., et al. (2010). Phosphorylation by Cdk2 is required for Myc to repress Ras-induced senescence in cotransformation. *Proc. Natl. Acad. Sci. USA* 107, 58–63.
- Kieffer-Kwon, K.R., Nimura, K., Rao, S.S.P., Xu, J., Jung, S., Pekowska, A., Dose, M., Stevens, E., Mathe, E., Dong, P., et al. (2017). Myc Regulates Chromatin Decompaction and Nuclear Architecture during B Cell Activation. *Mol. Cell* 67, 566–578.
- Knoepfler, P.S. (2008). Why myc? An unexpected ingredient in the stem cell cocktail. *Cell Stem Cell* 2, 18–21.
- Kress, T.R., Sabò, A., and Amati, B. (2015). MYC: connecting selective transcriptional control to global RNA production. *Nat. Rev. Cancer* 15, 593–607.
- Li, R., Liang, J., Ni, S., Zhou, T., Qing, X., Li, H., He, W., Chen, J., Li, F., Zhuang, Q., et al. (2010). A mesenchymal-to-epithelial transition initiates and is required for the nuclear reprogramming of mouse fibroblasts. *Cell Stem Cell* 7, 51–63.
- Li, G., Ren, C., Shi, J., Huang, W., Liu, H., Feng, X., Liu, W., Zhu, B., Zhang, C., Wang, L., et al. (2013). Identification, expression and subcellular localization of ESRG. *Biochem. Biophys. Res. Commun.* 435, 160–164.
- Lin, Y.C., Hsieh, L.C., Kuo, M.W., Yu, J., Kuo, H.H., Lo, W.L., Lin, R.J., Yu, A.L., and Li, W.H. (2007). Human TRIM71 and its nematode homologue are targets of let-7 microRNA and its zebrafish orthologue is essential for development. *Mol. Biol. Evol.* 24, 2525–2534.
- Lin, C.H., Jackson, A.L., Guo, J., Linsley, P.S., and Eisenman, R.N. (2009). Myc-regulated microRNAs attenuate embryonic stem cell differentiation. *EMBO J.* 28, 3157–3170.
- Lin, C.Y., Lovén, J., Rahl, P.B., Paranal, R.M., Burge, C.B., Bradner, J.E., Lee, T.I., and Young, R.A. (2012). Transcriptional amplification in tumor cells with elevated c-Myc. *Cell* 151, 56–67.
- Lu, X., Sachs, F., Ramsay, L., Jacques, P.E., Göke, J., Bourque, G., and Ng, H.H. (2014). The retrovirus HERVH is a long noncoding RNA required for human embryonic stem cell identity. *Nat. Struct. Mol. Biol.* 21, 423–425.
- Muñoz-Espin, D., and Serrano, M. (2014). Cellular senescence: from physiology to pathology. *Nat. Rev. Mol. Cell Biol.* 15, 482–496.
- Nakagawa, M., Koyanagi, M., Tanabe, K., Takahashi, K., Ichisaka, T., Aoi, T., Okita, K., Mochizuki, Y., Takizawa, N., and Yamanaka, S. (2008). Generation of induced pluripotent stem cells without Myc from mouse and human fibroblasts. *Nat. Biotechnol.* 26, 101–106.
- Nakagawa, M., Takizawa, N., Narita, M., Ichisaka, T., and Yamanaka, S. (2010). Promotion of direct reprogramming by transformation-deficient Myc. *Proc. Natl. Acad. Sci. USA* 107, 14152–14157.
- O'Malley, J., Skylaki, S., Iwabuchi, K.A., Chantzoura, E., Ruetz, T., Johnsson, A., Tomlinson, S.R., Linnarsson, S., and Kaji, K. (2013). High-resolution analysis with novel cell-surface markers identifies routes to iPS cells. *Nature* 499, 88–91.
- Ohnuki, M., Tanabe, K., Sutou, K., Teramoto, I., Sawamura, Y., Narita, M., Nakamura, M., Tokunaga, Y., Watanabe, A., Yamanaka, S., et al. (2014). Dynamic regulation of human endogenous retroviruses mediates factor-induced reprogramming and differentiation potential. *Proc. Natl. Acad. Sci. USA* 111, 12426–12431.
- Peukert, K., Staller, P., Schneider, A., Carmichael, G., Hänel, F., and Eilers, M. (1997). An alternative pathway for gene regulation by Myc. *EMBO J.* 16, 5672–5686.
- Polo, J.M., Anderssen, E., Walsh, R.M., Schwarz, B.A., Nefzger, C.M., Lim, S.M., Borkent, M., Apostolou, E., Alaei, S., Cloutier, J., et al. (2012). A molecular roadmap of reprogramming somatic cells into iPS cells. *Cell* 151, 1617–1632.
- Slack, F.J., Basson, M., Liu, Z., Ambros, V., Horvitz, H.R., and Ruvkun, G. (2000). The lin-41 RBCC gene acts in the *C. elegans* heterochronic pathway between the let-7 regulatory RNA and the LIN-29 transcription factor. *Mol. Cell* 5, 659–669.
- Smith, K.N., Singh, A.M., and Dalton, S. (2010). Myc represses primitive endoderm differentiation in pluripotent stem cells. *Cell Stem Cell* 7, 343–354.
- Soufi, A., Donahue, G., and Zaret, K.S. (2012). Facilitators and impediments of the pluripotency reprogramming factors' initial engagement with the genome. *Cell* 151, 994–1004.
- Sridharan, R., Tchieu, J., Mason, M.J., Yachechko, R., Kuoy, E., Horvath, S., Zhou, Q., and Plath, K. (2009). Role of the murine reprogramming factors in the induction of pluripotency. *Cell* 136, 364–377.
- Takahashi, K., and Yamanaka, S. (2006). Induction of pluripotent stem cells from mouse embryonic and adult fibroblast cultures by defined factors. *Cell* 126, 663–676.
- Takahashi, K., Tanabe, K., Ohnuki, M., Narita, M., Ichisaka, T., Tomoda, K., and Yamanaka, S. (2007). Induction of pluripotent stem cells from adult human fibroblasts by defined factors. *Cell* 131, 861–872.
- Takahashi, K., Tanabe, K., Ohnuki, M., Narita, M., Sasaki, A., Yamamoto, M., Nakamura, M., Sutou, K., Osafune, K., and Yamanaka, S. (2014). Induction of pluripotency in human somatic cells via a transient state resembling primitive streak-like mesendoderm. *Nat. Commun.* 5, 3678.
- Utikal, J., Polo, J.M., Stadtfeld, M., Maherali, N., Kulal, W., Walsh, R.M., Khalil, A., Rheinwald, J.G., and Hochedlinger, K. (2009). Immortalization eliminates a roadblock during cellular reprogramming into iPS cells. *Nature* 460, 1145–1148.
- van Lohuizen, M., Verbeek, S., Scheijen, B., Wientjens, E., van der Gulden, H., and Berns, A. (1991). Identification of cooperating oncogenes in E mu-myc transgenic mice by provirus tagging. *Cell* 65, 737–752.
- Varum, S., Rodrigues, A.S., Moura, M.B., Momcilovic, O., Easley, C.A., 4th, Ramalho-Santos, J., Van Houten, B., and Schatten, G. (2011). Energy metabolism in human pluripotent stem cells and their differentiated counterparts. *PLoS ONE* 6, e20914.
- Vennstrom, B., Sheiness, D., Zabielski, J., and Bishop, J.M. (1982). Isolation and characterization of c-myc, a cellular homolog of the oncogene (v-myc) of avian myelocytomatosis virus strain 29. *J. Virol.* 42, 773–779.
- Vervoorts, J., Lüscher-Firzlaff, J.M., Rottmann, S., Lilischkis, R., Walsemann, G., Dohmann, K., Austen, M., and Lüscher, B. (2003). Stimulation of c-MYC transcriptional activity and acetylation by recruitment of the cofactor CBP. *EMBO Rep.* 4, 484–490.
- Wang, J., Xie, G., Singh, M., Ghanbarian, A.T., Raskó, T., Szvetnik, A., Cai, H., Besser, D., Prigione, A., Fuchs, N.V., et al. (2014). Primate-specific endogenous retrovirus-driven transcription defines naive-like stem cells. *Nature* 516, 405–409.
- Wernig, M., Meissner, A., Cassady, J.P., and Jaenisch, R. (2008). c-Myc is dispensable for direct reprogramming of mouse fibroblasts. *Cell Stem Cell* 2, 10–12.
- Wolf, E., Lin, C.Y., Eilers, M., and Levens, D.L. (2015). Taming of the beast: shaping Myc-dependent amplification. *Trends Cell Biol.* 25, 241–248.
- Woodward, G.E., and Hudson, M.T. (1954). The effect of 2-deoxy-D-glucose on glycolysis and respiration of tumor and normal tissues. *Cancer Res.* 14, 599–605.
- Worringer, K.A., Rand, T.A., Hayashi, Y., Sami, S., Takahashi, K., Tanabe, K., Narita, M., Srivastava, D., and Yamanaka, S. (2014). The let-7/LIN-41 pathway regulates reprogramming to human induced pluripotent stem cells by controlling expression of prodifferentiation genes. *Cell Stem Cell* 14, 40–52.